

1-1-1975

# The Effective Autocorrelation Function of Maximum Entropy Spectra

Richard E. DuBroff

Missouri University of Science and Technology, red@mst.edu

Follow this and additional works at: [http://scholarsmine.mst.edu/ele\\_comeng\\_facwork](http://scholarsmine.mst.edu/ele_comeng_facwork)



Part of the [Electrical and Computer Engineering Commons](#)

---

## Recommended Citation

R. E. DuBroff, "The Effective Autocorrelation Function of Maximum Entropy Spectra," *Proceedings of the IEEE*, Institute of Electrical and Electronics Engineers (IEEE), Jan 1975.

The definitive version is available at <https://doi.org/10.1109/PROC.1975.10019>

This Article - Conference proceedings is brought to you for free and open access by Scholars' Mine. It has been accepted for inclusion in Electrical and Computer Engineering Faculty Research & Creative Works by an authorized administrator of Scholars' Mine. This work is protected by U. S. Copyright Law. Unauthorized use including reproduction for redistribution requires the permission of the copyright holder. For more information, please contact [scholarsmine@mst.edu](mailto:scholarsmine@mst.edu).

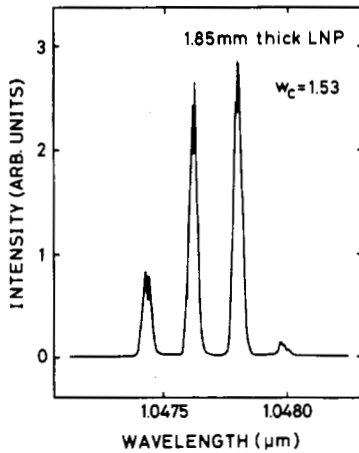


Fig. 3. Emission spectrum of 1.85-mm-thick LNP at  $w_c = 1.53$ . Oscillating mode spacing is  $1.8_\text{Å}$ .

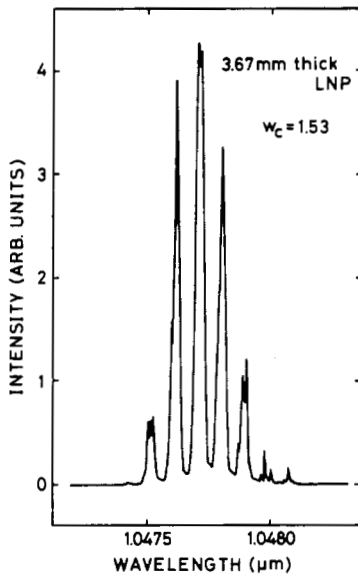


Fig. 4. Emission spectrum of 3.67-mm-thick LNP at  $w_c = 1.53$ . Oscillating mode spacing is  $0.9_\text{Å}$ .

The oscillating mode spectrum was analyzed with a JASCO single grating spectrometer with a resolution of  $0.1 \text{ Å}$ . A cooled  $S-1$  photomultiplier and a lock-in amplifier were used to record the laser spectrum.

Fig. 2 shows the measured output spectrum at various pump powers, where  $w_c$  is the relative pump power  $P/P_{th}$ . It is found that the laser oscillates in 1 longitudinal mode. This is due to the etalon effect of the crystal. Since the free spectral range of the etalon of  $0.3\text{-mm}$  thickness is  $12 \text{ Å}$  and the fluorescence linewidth of LNP is  $17 \text{ Å}$  [7], the second longitudinal mode is out of the gain curve and the single-longitudinal mode is kept sufficiently at typical pump levels.

To confirm the etalon effect of the crystal, we pumped  $1.85\text{-mm}$  and  $3.67\text{-mm}$ -thick LNP crystals in the same cavity configuration. The results are shown in Figs. 3 and 4. The emission spectrum consists of multilongitudinal modes separated by  $\Delta\lambda = 1.8_\text{Å}$  for the  $1.85\text{-mm}$ -thick crystal and  $\Delta\lambda = 0.9_\text{Å}$  for the  $3.67\text{-mm}$ -thick crystal. The mode spacing coincides with that resulting from the mode selecting laser crystal. The bandwidth of the spectrum increased with pump power initially, then decreased to the constant value of about  $2 \text{ Å}$  for both crystals. This is probably due to the saturation effect of the population in the  $^4F_{3/2}$  manifold at the steady state.

Despite the fast energy diffusion due to the high Nd ion density, the second mode appeared as soon as threshold was reached. Adopting numerical values from Nd:YAG [8] and extrapolating for LNP using the spectroscopic data [7], the diffusion distance is calculated to be about  $4400 \text{ Å}$ , which is longer than a quarter-wavelength of the  $1.0477\text{-}\mu\text{m}$  line inside the LNP crystal ( $1658 \text{ Å}$ ). Therefore, one would

consequently expect spontaneous single frequency operation for pumping up to 6 times threshold in a CW LNP laser. However, the observed multimode operation in these thick crystals shows that the spatial diffusion in LNP is slower than the theoretical estimation and is not sufficient to result spontaneous single frequency operation.

In conclusion, we have demonstrated the CW single-longitudinal-mode operation in the  $0.3\text{-mm}$ -thick LNP laser, using the frequency selecting effect of the crystal. With the pump power of  $8 \text{ mW}$  at  $5145 \text{ Å}$ , which is 6.5 times the threshold, the output power of the desired single mode was  $2.2 \text{ mW}$ . However, the emission spectrum in the LNP crystal of the thickness over  $1 \text{ mm}$  consisted of multilongitudinal modes as a consequence of the spatial hole burning effect, and single-mode operation was not observed.

Single-longitudinal-mode operation is of great interest because of the prospect of compact miniature laser pumped longitudinally with a light emitting diode.

#### ACKNOWLEDGMENT

The authors wish to thank Dr. N. Nüzeki and Dr. H. Iwasaki for their encouragement and valuable criticism.

#### REFERENCES

- [1] C. L. Tang, H. Statz, and G. DeMars, "Spectral output and spiking behavior of solid-state lasers," *J. Appl. Phys.*, vol. 126, pp. 580-593, Apr. 1962.
- [2] T. Kimura, K. Otsuka, and M. Saruwatari, "Spatial hole-burning effects in a  $\text{Nd}^{3+}$ :YAG laser," *IEEE J. Quantum Electron.*, vol. QE-7, pp. 225-230, June 1971.
- [3] H. Gerhardt, V. Bödecker, and H. Welling, "Frequency behavior of a frequency-stable YAG:  $\text{Nd}^{3+}$  laser" (in German), *Z. angew. Phys.*, vol. 31, pp. 11-15, Jan. 1, 1971.
- [4] P. W. Smith, M. V. Schneider, and H. G. Danielmeyer, "High-power single-frequency lasers using thin metal films mode-selection filters," *Bell Syst. Tech. J.*, vol. 48, pp. 1405-1419, May-June 1969.
- [5] W. Culshaw and J. Kannelaud, "Two-component-mode filters for optimum single-frequency operation of Nd:YAG lasers," *IEEE J. Quantum Electron.*, vol. QE-7, pp. 381-387, Aug. 1971.
- [6] D. A. Draeger, "Efficient single-longitudinal-mode Nd:YAG laser," *IEEE J. Quantum Electron.*, vol. QE-8, pp. 235-239, Feb. 1972.
- [7] K. Otsuka, T. Yamada, M. Saruwatari, and T. Kimura, "Spectroscopy and laser oscillation properties of lithium neodymium tetraphosphate," *IEEE J. Quantum Electron.*, vol. QE-11, pp. 330-335, July 1975.
- [8] H. G. Danielmeyer, M. Blätte, and P. Balmer, "Fluorescence quenching in Nd:YAG," *Appl. Phys.*, vol. 1, pp. 269-274, May 1973.

### The Effective Autocorrelation Function of Maximum Entropy Spectra

RICHARD E. DUBROFF

**Abstract**—The technique and the relative advantages of maximum entropy spectrum analysis have been discussed by Burg [1]; [2]. Evaluation of the inverse Fourier transform of the maximum entropy spectrum shows that this method does, indeed, correspond to a reasonable nonzero extension of the autocorrelation function.

#### I. INTRODUCTION AND NOTATION

The maximum entropy power spectrum may, in theory, be constructed by the following procedure, as has been shown by Burg [1], [2] and Barnard [3]. The known values of the autocorrelation function  $\phi_{xx}(\tau)$  of a zero mean random process  $x$  at  $N$  equally spaced lags are used to construct an autocorrelation matrix  $\tilde{\Phi}$ , according to  $\Phi_{mn} = \phi_{xx}[(m-n)\Delta\tau]$  for all  $m$  and all  $n \in [1, N+1]$ . If we define  $\tilde{\Gamma}$  and  $\tilde{P}$  as  $N+1$  dimensional row vectors according to  $\tilde{\Gamma} \equiv [1, \Gamma_1, \Gamma_2, \Gamma_3, \dots, \Gamma_N]$ , and  $\tilde{P} \equiv [P_N, 0, 0, \dots, 0]$ , then the quantities  $\Gamma_1$  through  $\Gamma_N$  and  $P_N$  may be determined by solving

$$\tilde{\Gamma} \cdot \tilde{\Phi} = \tilde{P}. \quad (1)$$

The vector  $\tilde{\Gamma}$  is frequently referred to as the prediction error filter [1], since the convolution of  $\tilde{\Gamma}$  with the sampled process  $x_i$ , which is given by  $x_i + \sum_{k=1}^N \Gamma_k x_{i-k}$ , is the error in estimating  $x_i$  from a minimum

Manuscript received April 17, 1975; revised May 19, 1975. This work was supported in part by U.S. Air Force Grant F19628-74-C0044. The author is with the Department of Electrical Engineering, Ionosphere Radio Laboratory, University of Illinois, Urbana, Ill. 61801.

mean-square error linear combination of  $N$  preceding values of  $x_i$ . Having determined  $\hat{r}$ , the maximum entropy power spectrum,  $S(f)$  is given by

$$S(f) = \frac{\beta}{(\hat{z} \cdot \hat{r}^H)(\hat{r} \cdot \hat{z}^H)} \quad (2)$$

where the superscript  $H$  denotes the complex conjugate transpose;  $Z \equiv e^{j\omega\Delta\tau}$ ;  $\hat{z} \equiv [Z^0, Z^1, Z^2, \dots, Z^N]$ ; and  $\beta$  is a constant. The fact [3] that  $(\hat{z} \cdot \hat{r}^H)$  is never zero for  $|Z| < 1$ , and that  $(\hat{r} \cdot \hat{z}^H)$  is never zero for  $|Z| > 1$  will be used later.

The following section will show that the inverse Fourier transform of (2) is given by

$$\int_{\text{NB}} S(f) e^{j\omega k \Delta\tau} df = \phi_A(k\Delta\tau), \quad \text{for all integers } k \quad (3)$$

where NB = Nyquist band, and  $\phi_A(k\Delta\tau)$  is recursively constructed as

$$\phi_A(k\Delta\tau) \equiv \begin{cases} \phi_{xx}(k\Delta\tau), & \text{for } 0 < k \leq N \\ -\sum_{n=1}^N \Gamma_n \phi_A[(k-n)\Delta\tau], & \text{for } k > N \end{cases} \quad (4)$$

and, of course,  $\phi_A$  is an even function. Note that the effective autocorrelation function  $\phi_A$  agrees with  $\phi_{xx}$  when  $|k| \leq N$  and appears to be an extension of  $\phi_{xx}$  when  $|k| > N$ .

II. INVERSE FOURIER TRANSFORM OF SPECTRUM

We introduce the following definitions:

$$Z \equiv e^{j\omega\Delta\tau} \quad (5)$$

$$\hat{z}_K \equiv [Z^0, Z^1, Z^2, \dots, Z^K], \quad \text{for } K > N$$

(a  $K + 1$  dimensional row vector) (6)

$$\hat{r}_{N,K} \equiv [1, \Gamma_1, \Gamma_2, \dots, \Gamma_N, 0, \dots, 0], \quad \text{for } K > N$$

(a  $K + 1$  dimensional row vector) (7)

$$X_K \equiv \int_{\text{NB}} S(f) e^{j\omega K \Delta\tau} df, \quad \text{for } K > N \quad (8)$$

and, in addition, we define  $\tilde{Q}(K)$  as a  $(K + 1) \times (K + 1)$  matrix according to

$$Q_{mn}(K) \equiv \begin{cases} \phi_A[(m-n)\Delta\tau], & \text{when } 0 \leq |m-n| \leq K-1 \\ X_K, & \text{when } |m-n| = K \end{cases} \quad (9)$$

for all  $m \in [1, K + 1]$  and all  $n \in [1, K + 1]$ .

In order to prove (3) when  $k = N + 1$ , it is sufficient to show that  $X_{N+1} = \phi_A[(N + 1)\Delta\tau]$ . Since  $S(f)$  must satisfy a set of constraint equations [1], [2], which can be obtained by considering (3) for  $|k| \leq N$ , we may incorporate (8) into (3) by using (8), (9), and (5) for  $K = N + 1$ , and we find that

$$Q_{mn}(N + 1) = \int_{\text{NB}} S(f) Z^{(m-n)} df \quad (10)$$

which may be written in a matrix form, similar to the form used by Barnard [3], as

$$\tilde{Q}(N + 1) = \frac{\beta}{2\pi j \Delta\tau} \oint \frac{\hat{z}_{N+1}^H \hat{z}_{N+1} dZ}{Z(\hat{z}_{N+1} \cdot \hat{r}_{N,N+1}^H)(\hat{r}_{N,N+1} \cdot \hat{z}_{N+1}^H)} \quad (11)$$

where the path of integration is the unit circle in the  $z$  plane. Premultiplying (11) by  $\hat{r}_{N,N+1}^H$ , cancelling common factors in the integrand, and noting that  $(\hat{z}_{N+1} \cdot \hat{r}_{N,N+1}^H)$  is never zero inside the unit circle, the last column of (11) becomes

$$X_{N+1} + \sum_{n=1}^N \Gamma_n \phi_A[(N + 1 - n)\Delta\tau] = \frac{\beta}{2\pi j \Delta\tau} \oint \frac{Z^N dZ}{(\hat{z}_{N+1} \cdot \hat{r}_{N,N+1}^H)} = 0. \quad (12)$$

Comparing (12) with (4) indicates that  $X_{N+1} = \phi_A[(N + 1)\Delta\tau]$ .

The next step in the inductive proof of (3) is to assume that (3) is valid when  $|k| < M$ , and show that (3) is also valid when  $|k| = M + 1$ . It is sufficient to show that

$$X_{M+1} = \phi_A[(M + 1)\Delta\tau] \quad (13)$$

by evaluating

$$\tilde{Q}(M + 1) = \frac{\beta}{2\pi j \Delta\tau} \oint \frac{\hat{z}_{M+1}^H \hat{z}_{M+1} dZ}{Z(\hat{z}_{M+1} \cdot \hat{r}_{N,M+1}^H)(\hat{r}_{N,M+1} \cdot \hat{z}_{M+1}^H)} \quad (14)$$

The evaluation of (14) is entirely analogous to the evaluation of (11). Therefore, after multiplying both sides of (14) by  $\hat{r}_{N,M+1}^H$  and considering only the last column of the resulting equation, it is found that

$$X_{M+1} + \sum_{n=1}^N \Gamma_n \phi_A[(M + 1 - n)\Delta\tau] = 0. \quad (15)$$

Comparison with (4) indicates that  $X_{M+1} = \phi_A[(M + 1)\Delta\tau]$ .

III. CONCLUSION

The validity of (3) is not surprising in light of the recent work of Ulrych and Bishop [4], since  $\phi_A(k\Delta\tau)$  is essentially the result of using the prediction error filter to predict future values of the autocorrelation function. It is also interesting to note that in spite of the fact that maximum entropy spectra correspond to an infinitely long autocorrelation function, it is still possible to compute these spectra using a finite number of operations, as shown by (2). This result contrasts sharply with the conventional power spectrum analysis [5] in which the window function causes the inverse Fourier transform of the spectrum to be nonzero only over a finite length of time, thereby causing sidelobes to appear in the conventional spectrum, as noted by Burg [1].

ACKNOWLEDGMENT

The author would like to thank Dr. K. C. Yeh for his interest and encouragement in this work.

REFERENCES

- [1] J. P. Burg, "Maximum entropy spectral analysis," presented at the 37th Annu. Int. SEG Meeting, Oklahoma City, Okla., Oct. 1967.
- [2] —, "A new analysis technique for time series data," presented at the NATO Advanced Study Inst. Signal Processing with Emphasis on Underwater Acoustics, Enschede, Netherlands, 1968.
- [3] T. E. Barnard, "Analytical studies of techniques for the computation of high-resolution wavenumber spectra," Science Services Division, Texas Instruments, Inc., Dallas, Tex., Special Rep. 9, May 14, 1969.
- [4] T. J. Ulrych and T. N. Bishop, "Maximum entropy spectral analysis and autoregressive decomposition," *Rev. Geophys. Space Phys.*, vol. 13, pp. 183-200, Feb. 1975.
- [5] R. B. Blackman and J. W. Tukey, *The Measurement of Power Spectra From the Point of View of Communications Engineering*. New York: Dover, 1959.

An Alternate Derivation of the Maximum Likelihood Estimator of a Covariance Matrix

RAMON NITZBERG

**Abstract**—An alternate derivation of the maximum likelihood estimator of a covariance matrix is given. The derivation is based upon the eigenvalue properties of the product of the inverse of the covariance matrix and the sample covariance matrix.

Manuscript received April 24, 1975.

The author is with Advanced Systems and Technology, Electronic Systems Division, General Electric Company, Syracuse, N.Y. 13201.